Plant Physiol. (1989) 91, 331–337
0032-0889/89/91/0331/07/$01.00/0

Received for publication February 13, 1989
and in revised form April 17, 1989

Chlorophyll *a* Fluorescence Predicts Total Photosynthetic Electron Flow to CO_2 or NO_3^-/NO_2^- under Transient Conditions[1]

Jody J. Holmes, Harold G. Weger, and David H. Turpin*

Department of Biology, Queen's University, Kingston, Ontario, Canada, K7L 3N6

ABSTRACT

A model which predicts total photosynthetic electron flow from a linear regression of the relationship between corrected steady-state quantum yield and nonphotochemical quenching (E Weis, JA Berry [1987] Biochem Biophys Acta 894: 198–208) was formulated for *N*-limited cells of the green alga *Selenastrum minutum*. Unlike other models based on net CO_2 fixation, our model is based on total photosynthetic electron flow measured as gross O_2 evolution. This allowed for the prediction of total photosynthetic electron flow from water to both CO_2 fixation and NO_3^-/NO_2^- reduction. The linear regression equation predicting electron flow is of the form: $J = I \cdot Q_q[0.4777-0.3282\ Q_{NP}]$ (where J = gross photosynthetic electron flow, I = incident PAR, Q_q = photochemical quenching, Q_{NP} = nonphotochemical quenching). During steady-state photosynthesis, over a range of irradiance, the model predicted a photosynthetic light saturation curve which was well correlated with that observed. Although developed under steady-state conditions, the model was tested during non-steady-state photosynthesis induced by transient nitrogen assimilation. The model predicted transient rates of gross O_2 evolution which were in excellent agreement with the rates observed under a variety of conditions regardless of whether CO_2 or NO_3^-/NO_2^- served as the physiological electron acceptor. The fluorescence transients resulting from ammonium and nitrate assimilation are discussed with respect to metabolic demands for reductant and ATP.

Chlorophyll *a* fluorescence provides a sensitive indicator of photochemical processes (12, 14). Qualitative relations between fluorescence emission and photochemistry have frequently been demonstrated, but these relations have been obscured by the fact that there are two major mechanisms of fluorescence quenching (10, 13). Differentiation of these mechanisms via the light doubling procedure of Bradbury and Baker (2, 3) and subsequent development of the 'saturation pulse' method (22) and modulation techniques (9, 15, 20, 22) have allowed the formulation of models predicting rates of photosynthetic electron transport based upon quenching analysis of fluorescence emission (22, 31, 32). Quenching of chl *a* fluorescence emission can occur as a result of changes in the redox level of Q_A, the primary electron acceptor of PSII (photochemical quenching; Q_q). Oxidized Q_A allows excitation energy to be used for photochemistry, preventing the reemission of light energy as fluorescence (*i.e.* 'quenching' the fluorescence). Quenching may also result from nonphotochemical processes (nonphotochemical quenching; Q_{NP}). Although there are potentially several mechanisms accounting for Q_{NP}, it is generally believed that increases in the transthylakoid pH gradient may result in structural changes which are thought to increase thermal dissipation of absorbed light energy. While Q_q is a measure of the oxidation state of Q_A, and therefore one indicator of the ability of PSII to utilize excitation energy to perform work, it has been repeatedly shown that Q_{NP} quenching is negatively correlated with quantum yield of PSII (10, 11, 17, 18, 31, 32). This suggests an important role for thylakoid membrane energization in the regulation of PSII activity. Thus, models for the estimation of photosynthetic electron transport from fluorescence must take into account both of these quenching mechanisms.

Weis and Berry (31) have shown that quenching analysis can be used to estimate total electron transport rates (J) from fluorescence emission according to the equation:

$$J = I \cdot Q_q(b - mQ_{NP})$$

where I is the incident PAR, and m and b are empirically derived constants. Rates of steady-state photosynthetic electron transport calculated using these fluorescence-derived parameters were highly correlated to electron transport rates calculated from net CO_2 exchange (23, 31, 32).

In this report we utilize gross photosynthetic O_2 evolution, measured via mass spectrometry, to derive the constants m and b, and to confirm fluorescence-based estimates the total photosynthetic electron transport chain activity. Use of gross O_2 evolution as a measure of photosynthetic electron flow is an improvement over net CO_2 exchange as it is not biased by respiratory CO_2 release. More importantly, it facilitates the measurement of photosynthetic electron transport to substrates other than CO_2, such as inorganic nitrogen. We show that fluorescence-based estimates of electron transport provide an accurate measure of photosynthetic electron flow, regardless of the electron acceptor (CO_2 or NO_3^-/NO_2^-), during both steady-state and transient photosynthesis.

MATERIALS AND METHODS

Organism and Culture

The green alga, *Selenastrum minutum* Naeg. Collins (UTEX 2459) was grown axenically in chemostat culture

[1] Supported by the Natural Sciences and Engineering Research Council of Canada. HGW acknowledges an Ontario Graduate Scholarship.

under NO_3^- limitation at a growth rate of 0.3 d^{-1}. Complete culture conditions were as described in Elrifi and Turpin (4).

Experimental

Cells were harvested from chemostats and resuspended at a density of approximately 30 μg Chl mL^{-1} in DIC-free, N_2-sparged Na-HEPES (pH 7.0, 25 mM). Gross photosynthetic O_2 evolution and CO_2 fixation were measured with a VG Gas Analysis MM14-80SC mass spectrometer (Middlewich, England) as previously described (29). Mass/charge (m/z) ratios of 32($^{16}O_2$), 36($^{18}O_2$), 40(^{40}Ar), 44($^{12}CO_2$), and 45($^{13}CO_2$) were measured once every 12 s. Rates of gross O_2 and CO_2 exchange were calculated according to Peltier and Thibault (16) and Turpin *et al.* (27).

Measurements of Fluorescence

Fluorescence was monitored using a PAM fluorometer (Heinz Walz, Effeltrich, FRG) with the fiber optic cable connected directly to the mass spectrometer cuvette (26). Detailed explanation of the operation of this system can be found elsewhere (21, 22). Briefly, a low intensity measuring beam pulses at a specific frequency (100 or 1.6 kHz). Only the fluorescence emission stimulated by this beam is amplified. Thus, changes in actinic light intensity do not affect measurement of changes in photochemistry.

For determination of F_0 (the minimum level of fluorescence), cells were allowed to dark adapt for 5 min and fluorescence measured at 1.6 kHz. The maximum variable fluorescence, $(Fv)_{max}$, was measured by switching the modulation frequency to 100 kHz and then immediately applying a saturating pulse of light to dark-adapted cells. Following F_0 determination cells were illuminated with a 300 W projector lamp (General Electric). To examine the effects of different levels of PAR, neutral density filters were used. During N-pulsing experiments, PAR was 490 μmol quanta m^{-2} s^{-1}. Irradiance was measured as PAR incident on the proximal glass surface of the mass spectrometer cuvette. In the light, saturating pulses of 1 second duration were applied every 10 s to fully reduce Q_A, allowing determination of flash saturated variable fluorescence, $(F_v)_s$. F_v (variable fluorescence in the absence of a flash) and $(F_v)_s$ were monitored continuously throughout the nitrogen induced transients. Quenching of F_0 during photosynthesis (1, 18, 31) may occur under some conditions. This was determined by turning off the actinic light and switching to 1.6 kHz for a period of 1 s (1, 10, 17).

Calculation of Quenching Coefficients

Q_q and Q_{NP} were calculated using the equations of Schreiber *et al.* (22):

$$Q_{NP} = \frac{(F_v)_{max} - (F_v)_s}{(F_v)_{max}}$$

$$Q_q = \frac{(F_v)_s - F_v}{(F_v)_s}.$$

Inorganic Nitrogen Analysis

Nitrogen was added to cells 1 min after the establishment of steady-state fluorescence as either NH_4Cl or $NaNO_3$. Final concentrations ranged from 50 to 750 μM. Aliquots (1.0 mL) of cells were taken at discrete intervals throughout nitrogen-induced transients and immediately frozen in liquid N_2. Samples were subsequently thawed and refrozen twice to permeabilize membranes, centrifuged, and then analyzed for total NO_3^- + NO_2^- content according to Strickland and Parsons (25). Ammonium was also analyzed but remained low throughout the experiments, consequently NO_3^-/NO_2^- disappearance reflected N assimilation.

Other Measurements

Chl was measured by extraction in methanol (8).

RESULTS

Development of the Model

The analysis was as described by Weis and Berry (31), except that gross O_2 evolution was used as the measure of photosynthetic electron transport rather than net CO_2 fixation. The model is based on the premise that apparent quantum yield should be proportional to changes in Q_q, and that the remaining variation should be proportional to Q_{NP}. Φ_s is defined as the electron flow necessary to support observed rates of gross O_2 evolution, relative to the incident PAR. Φ_s can be corrected for the effects of closed reaction centers, such that the corrected apparent quantum yield ($\Phi_p = \Phi_s/q_q$) is an estimate of the quantum yield if all reaction centers are open.

By applying linear regression analysis, the relationship between Φ_p and Q_{NP} (Fig. 1) can be used to derive the parameters m and b in Equation 1 where $m = \Phi_{po} - \Phi_{pl}$, and $b = \Phi_{po}$. Φ_{po} and Φ_{pl} are obtained from Figure 1 where $Q_{NP} = 0$ and $Q_{NP} = 1$, respectively. With these empirically derived parameters, the rate of electron transport indicated by fluorescence quenching analysis can be calculated from

$$J = I \cdot Q_q[0.4177 - 0.3282\ Q_{NP}]. \quad (1)$$

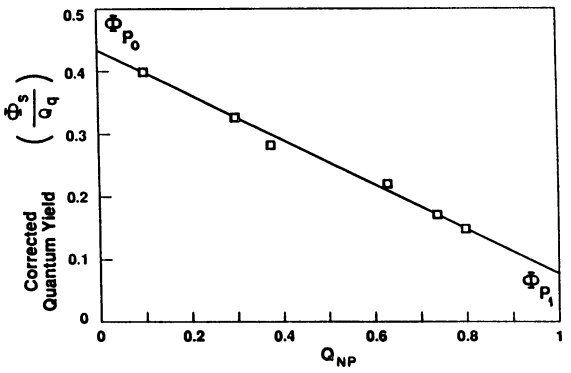

Figure 1. Dependence of corrected quantum yield (Φ_s/Q_q) on Q_{NP}. Data points are calculated from steady-state rates of electron flow measured as gross O_2 evolution. Q_{NP} was varied via changes in incident PAR.

For further details of the derivation of this equation, see Weis and Berry (31), and Weis *et al.* (32).

Predictions of the Model under Steady-State Conditions

The model relationship (Eq. 1) was used to calculate rates of steady-state photosynthetic electron flow from fluorescence quenching coefficients at different levels of PAR. Rates of electron transport estimated from the model correlated well with the rate of electron transport required to support the measured rate of gross O_2 evolution (Fig. 2).

Predictions of the Model During N-Induced Photosynthetic Transients

Effects of Ammonium Assimilation on Gross Gas Exchange and Fluorescence Quenching

Addition of NH_4^+ (200 μM) to *N*-limited *S. minutum* during steady-state photosynthesis resulted in large changes in fluorescence and photosynthetic gas exchange as previously reported (4, 5, 26, 27, 30). In particular, NH_4^+ addition resulted in a transient suppression of photosynthetic O_2 evolution and CO_2 fixation as well as a peak in Q_{NP} followed by a decline in both Q_q and Q_{NP} (Fig. 3). Gross CO_2 fixation, O_2 evolution, Q_{NP} and Q_q recovered when all the added NH_4^+ was assimilated (ammonium assimilation data is not shown, see ref. 26). The rate of O_2 evolution necessary to support electron flow, as predicted from values of fluorescence quenching and Equation 1 are in excellent agreement with the observed levels of O_2 evolution (Fig. 3B).

Effects of Nitrate Assimilation on Gross Gas Exchange and Fluorescence Quenching

The addition of NO_3^- resulted in three distinct changes in fluorescence quenching (Fig. 4). First, Q_{NP} exhibited a 3 to 4 min period of oscillation before returning to a steady-state value. The duration of this oscillation was similar regardless

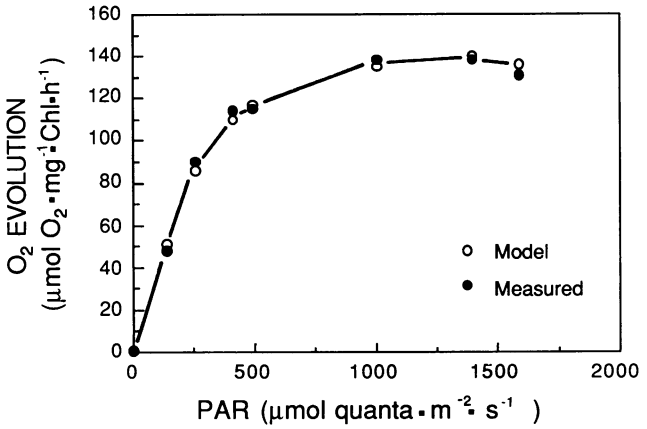

Figure 2. Comparison of predicted and observed levels of photosynthetic electron flow at various levels of PAR. Calculations of photosynthetic electron flow from Q_q and Q_{NP} and Equation 1 were made from measurements averaged over a 1 min period of steady-state photosynthesis at each light level. Water photolysis was measured simultaneously via mass spectrometry.

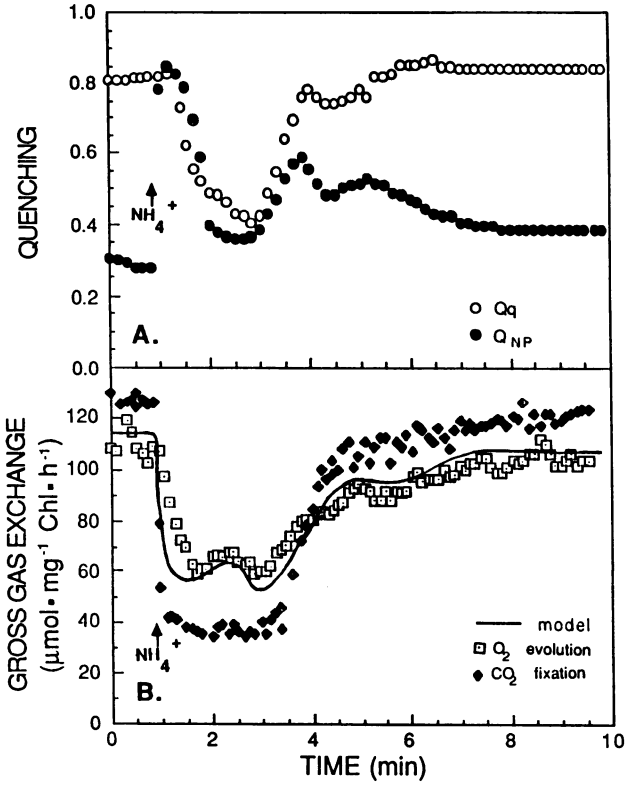

Figure 3. Effect of 200 μM NH_4^+ addition to *N*-limited *S. minutum* on quenching coefficients and gross photosynthetic O_2 evolution. A, Changes in Q_q and Q_{NP} during transient NH_4^+ assimilation. B, Simultaneous changes in gross photosynthetic O_2 evolution (□) and CO_2 fixation (♦). *Solid line* represents the model predictions of photosynthetic O_2 evolution based on Equation 1 and the values of Q_q and Q_{NP} reported in panel A.

of the NO_3^- concentration added (Fig. 4, A, B, and C). Second, Q_q was relatively unaffected until all the NO_3^- and NO_2^- had been assimilated, at which point it declined rapidly, recovering again within approximately 1 min (Fig. 4A). Thirdly, approximately 15 to 20 s after the Q_q decline, a peak in Q_{NP} was observed. The transients in both Q_{NP} and Q_q which occurred after NO_3^-/NO_2^- assimilation returned to new steady-state levels within 5 min.

Like the initial fluorescence transient, the final transient was also independent of added NO_3^- concentration. Increased concentration of added NO_3^- only affected the time between the initial and final fluorescence transients, reflecting the greater time required for the assimilation of the added N (Figs. 4 and 5).

Concomitant with the changes in fluorescence quenching, NO_3^- addition resulted in an immediate decline in carbon fixation from approximately 110 to 37 μmol CO_2 mg^{-1} Chl h^{-1}. Figure 6 shows this effect for an experiment carried out with 500 μM NO_3^- added. Although photosynthetic CO_2 fixation was severely inhibited, O_2 evolution remained at steady-state levels until all the NO_3^- was assimilated (approximately 8.5 min after the addition of NO_3^-). At that time where was a transient decline in both O_2 evolution and Q_q. Subsequently, CO_2 fixation and O_2 evolution returned to control rates coincidentally with the recovery of Q_q and Q_{NP}

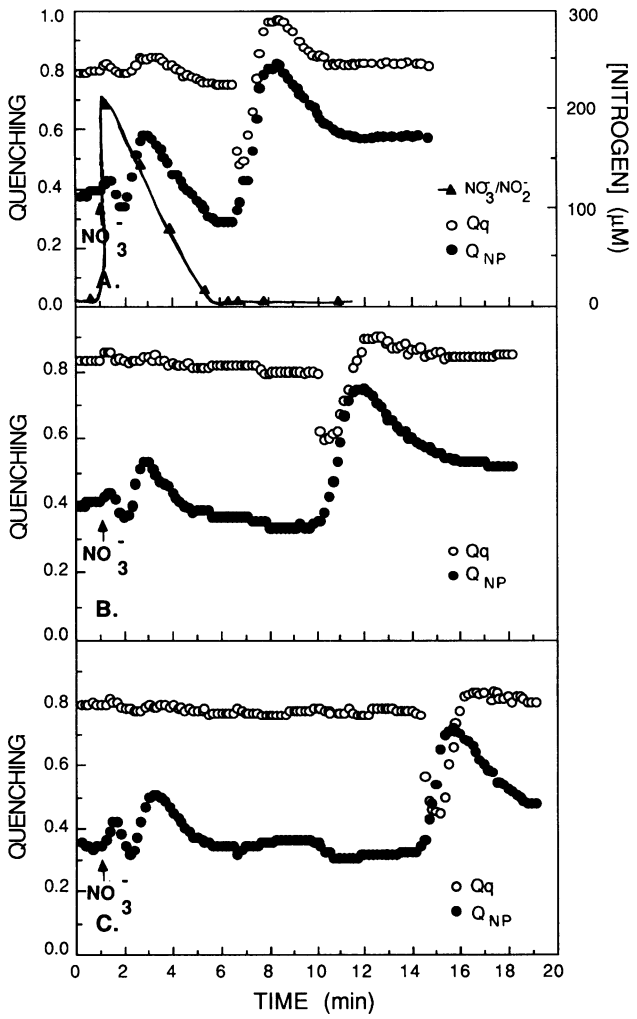

Figure 4. Effects of transient NO_3^- assimilation on quenching coefficients at three different NO_3^- concentrations: A, 250 μM; B, 500 μM; C, 750 μM. Panel A also shows a time course of NO_3^-/NO_2^- assimilation.

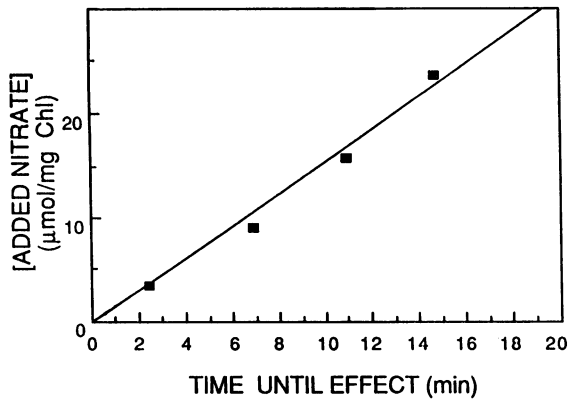

Figure 5. Effects of added NO_3^- concentration on the time until the beginning of the final Q_q and Q_{NP} transients.

(Fig. 6A). Using the model (Eq. 1), the observed changes in Q_q and Q_{NP} values yielded a prediction of gross O_2 evolution which was in excellent agreement with the experimental measurements of photosynthetic O_2 evolution (Fig. 6B).

Potential Sources of Error: F_0 Effects

Quenching of F_0 (Q_0) has been correlated with high levels of Q_{NP} (1, 18, 31). Since in our study Q_{NP} underwent a significant increase during both NH_4^+ and NO_3^- induced transients, it was necessary to examine F_0 quenching as a potential source of error in the calculation of quenching coefficients. Repeated F_0 determinations were made during both NO_3^- and NH_4^+ induced transients. Q_q and Q_{NP} were then recalculated as described by Bilger and Schreiber accounting for Q_0 (1). The quenching coefficients were not significantly different from those calculated using F_0 values determined following a dark period. Also they did not significantly affect the predicted rates of O_2 evolution.

DISCUSSION

Fluorescence Transients during N Assimilation

NH_4^+ Assimilation

Previous work on *N*-limited *S. minutum* has shown that transient NH_4^+ supply results in ribulose 1,5-bisphosphate limitation of photosynthetic carbon fixation (5), presumably due to increased requirements for carbon skeletons in the synthesis of amino acids (27). Most of the remaining carbon fixation is due to phosphoenolpyruvate carboxylase serving in an anaplerotic function by replenishing tricarboxylic acid cycle intermediates used in amino acid synthesis (7). The fact that there is still significant, although substantially decreased, photosynthetic O_2 evolution (Fig. 3) suggests photodriven electrons are providing reducing power to the glutamate synthase reaction. These changes in metabolism result in dramatic effects on fluorescence and O_2 evolution. The fluorescence transients reported in Fig. 3 are consistent with those reported by Turpin and Weger (26). These authors suggested that the decline in Calvin cycle ATP consumption was responsible for the initial increase in Q_{NP}. The subsequent Q_q decline was suggested to be a result of decreased NADPH consumption by glyceraldehyde 3-P dehydrogenase, and the ensuing decline in Q_{NP} was hypothesized to result from increased ATP consumption associated with N assimilation into amino acids and protein.

NO_3^-/NO_2^- Assimilation

The assimilation of NO_3^- by *N*-limited *S. minutum* also results in ribulose 1,5-bisphosphate limitation of photosynthetic carbon fixation (4, 5) and presumably much of the remaining carbon fixation is due to phospho*enol*pyruvate carboxylase (7). The reductant requirements for NO_3^-/NO_2^- reduction however, allow for maintenance of high rates of O_2 evolution (4, 29). This is illustrated in Figure 6 where NO_3^- assimilation resulted in a 70% decline in CO_2 fixation but no change in gross photosynthetic O_2 evolution until all added NO_3^- was assimilated. The absence of any effect on O_2

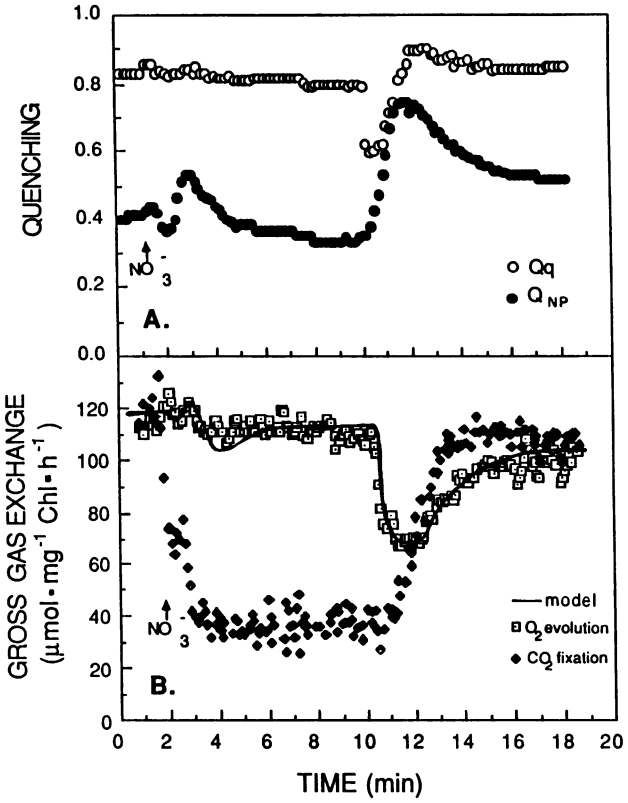

Figure 6. Effects of 500 μM NO_3^- addition to *N*-limited *S. minutum* on steady-state quenching coefficients and gross photosynthetic CO_2 fixation and O_2 evolution. A, Changes in Q_q and Q_{NP} during NO_3^--induced transients. B, Simultaneous changes in gross photosynthetic CO_2 fixation and O_2 evolution measured by mass spectrometry. *Solid line* represents the rate of O_2 evolution calculated from Equation 1 and the values of Q_q and Q_{NP} in panel A.

evolution implied a diversion of electron flow from CO_2 to NO_3^-/NO_2^- reduction (Fig. 6B). Since electron flow was maintained, photochemical quenching remained relatively unaffected (Fig. 6A). The oscillations in Q_{NP} following NO_3^- addition (Figs. 4 and 6) may reflect an equilibration between various ATP demanding reactions. In other words, when NO_3^- is first supplied Calvin cycle activity declines removing one ATP sink, but NO_3^- uptake and assimilation commence thereby introducing another. Following the complete assimilation of NO_3^-, but prior to the recovery of CO_2 fixation, pools of reduced Q_A accumulate resulting in a decrease in Q_q and water photolysis. Only when Calvin cycle induction has occurred, allowing the oxidation of Q_A, do Q_q and O_2 evolution recover (Fig. 6). The transient increase in Q_{NP} which follows the disappearance of NO_3^- and NO_2^- may be due to a decrease in the ATP required for N assimilation and peptide synthesis thus causing an increase in the transthylakoid proton gradient. As Calvin cycle activity recovers, ATP requirements increase and Q_{NP} returns to a steady-state level.

This induction process is similar to that observed upon illumination (19, 21, 24, 28). Following illumination, the electron transport chain is rapidly reduced resulting in a decline in Q_q. As the Calvin cycle is induced, the electron transport chain is oxidized and an increase in Q_q is observed. During induction, Q_{NP} also increases, reflecting an increase in membrane energization accompanying the low initial ATP demand. As the Calvin cycle is induced ATP consumption increases and Q_{NP} declines. It would appear that the analogous induction sequence occurs following periods of transient N assimilation and resultant ribulose 1,5-bisphosphate limitation of Calvin cycle activity in *N*-limited *S. minutum*.

Predicting Photosynthetic Electron Flow from Fluorescence Data

Predictions of Steady-State Photosynthesis

Changes in photochemical and nonphotochemical quenching affect the balance between absorbed quanta participating in photochemistry and those dissipated as heat or fluorescence. Incident light can have a large effect on this balance (18, 23, 31). When gross photosynthetic electron flow is plotted as a function of PAR, typical saturation kinetics are observed (Fig. 2). At low light, Calvin cycle activity and water photolysis are less than maximal. As incident light increases, photosynthesis becomes light saturated. This is reflected in the contributions of photochemical and nonphotochemical quenching at different light levels. At low light, Q_q quenching predominates because of the oxidized state of Q_A. At higher light the contribution of Q_q declines and nonphotochemical quenching (Q_{NP}) plays an increasingly important role (21, 31). There is mounting evidence that the decrease in quantum efficiency of PSII which occurs at high light intensity when Q_{NP} is high (Fig. 1) may reduce the likelihood of pigment damage through increased heat dissipation or the induction of state I-state II transitions *in vivo* (1, 18, 31).

By assuming that apparent quantum yield should be proportional to changes in photochemical quenching and then relating any remaining changes to nonphotochemical quenching, Weis and Berry (31) developed a model which predicts total electron flow from fluorescence measurements under steady-state conditions. Although some of the physiological mechanisms suggested in the development of this model have been criticized (6), this empirical model (Eq. 1), when calibrated with gross O_2 evolution, accurately predicts the light saturation curve from steady-state determinations of Q_q and Q_{NP} (Fig. 2).

Predictions during Transient Photosynthesis

Ideally, a model predicting photosynthetic electron flow from fluorescence measurements should be applicable under transient as well as steady-state conditions regardless of whether the electrons are used for CO_2 fixation or NO_3^-/NO_2^- reduction. The original model (31, 32) employed the assumption that photosynthetic electron flow was adequately reflected in net CO_2 assimilation. However, other processes such as nitrogen and sulfur assimilation are also photosynthetic processes. By using gross O_2 evolution as a direct measure of total photosynthetic electron flow, our derivation should be applicable regardless of the electron sink. A test of the model's utility under transient conditions was facilitated by examining the changes in photosynthesis which occur during N assimilation by *N*-limited *S. minutum*.

During NH_4^+ assimilation the demand for photosynthetic electron flow declines drastically. Using Equation 1 and the measured values of fluorescence quenching reported in Figure 3A, we obtained a prediction of photosynthetic electron flow which was in excellent agreement with observed rates (Fig. 3*B*). The observation that the decline in O_2 evolution laged several seconds behind the model prediction may be due to lags inherant in the measurement of gas exchange.

Transient NO_3^- assimilation tests the utility of the model during electron flow to acceptors other than CO_2. The predictions of photosynthetic electron flow under these conditions are also in excellent agreement with observed rates (Fig. 6). The model also provides an excellent prediction of the transient decline in photosynthetic electron flow which occurs following the complete assimilation of NO_3^-, prior to the induction of the Calvin cycle (Fig. 6).

CONCLUSION

We have calibrated the model developed by Weis and Berry (31) to predict gross photosynthetic electron flow from measurements of fluorescence quenching in *N*-limited *S. minutum*. This model provides an excellent prediction of photosynthetic electron flow under steady-state conditions and during photosynthetic transients induced by N assimilation. This model is also an accurate predictor of photosynthetic electron flow regardless of whether NO_3^-/NO_2^- or CO_2 serves as the terminal electron acceptor.

ACKNOWLEDGMENTS

We acknowledge Dr. J. T. Ball for suggesting that the *Selenastrum* system would provide an interesting test of the fluorescence model for calculating photosynthetic electron flow. We wish to thank Mr. D. G. Birch for aid in mass spectrometry, Dr. A. G. Miller for useful discussions and Drs. R. G. Smith and K. A. Schuller for reviewing the manuscript.

LITERATURE CITED

1. **Bilger W, Schreiber U** (1986) Energy-dependent quenching of dark-level chlorophyll fluorescence in intact leaves. Photosynth Res **10:** 303–308
2. **Bradbury M, Baker NR** (1981) Analysis of the slow phases in the *in vivo* chlorophyll fluorescence induction curve. Changes in the redox state of photosystem II electron acceptors and fluorescence emission from photosystem I and II. Biochem Biophys Acta **63:** 542–551
3. **Bradbury M, Baker NR** (1983) Analysis of the induction of chlorophyll fluorescence in leaves and isolated thylakoids: Contributions of photochemical and non-photochemical quenching. Proc R Soc Lond B **220:** 251–264
4. **Elrifi IR, Turpin DH** (1986) Nitrate and ammonium induced photosynthetic suppression in *N*-limited *Selenastrum minutum*. Plant Physiol **81:** 273–279
5. **Elrifi IR, Holmes JJ, Weger HG, Mayo WP, Turpin DH** (1988) RuBP limitation of photosynthetic carbon fixation during NH_3 assimilation: interactions between photosynthesis, respiration and ammonium assimilation in *N*-limited green algae. Plant Physiol **87:** 395–401
6. **Genty B, Briantais J-M, Baker NR** (1989) The relationship between the quantum yield of photosynthetic electron transport and quenching of chlorophyll fluorescence. Biochim Biophys Acta **990:** 87–92
7. **Guy RD, Vanlerberghe GC, Turpin DH** (1989) Significance of phospho*enol*pyruvate carboxylase during ammonium assimilation: carbon isotope discrimination in photosynthesis and respiration by the *N*-limited green alga *Selenastrum minutum*. Plant Physiol **89:** 1150–1157
8. **Holden M** (1976) Chlorophyll *a* and *b* determination. *In* TW Goodwin, ed, Chemistry and Biochemistry of Plant Pigments, Vol 2, Academic Press, London, pp 853–974
9. **Horton P** (1983) Relations between electron transport and carbon assimilation: simultaneous measurement of chlorophyll fluorescence, transthylakoid pH gradient and O_2 evolution in isolated chloroplasts. Proc R Soc Lond B **217:** 405–416
10. **Horton P, Hague A** (1988) Studies on the induction of chlorophyll fluorescence in isolated barley protoplasts. IV. Resolution of nonphotochemical quenching. Biochim Biophys Acta **932:** 107–115
11. **Krause GH, Laasch H** (1987) Energy-dependent chlorophyll fluorescence quenching in chloroplasts correlated with quantum yield of photosynthesis. Z Naturforsch **42c:** 581–584
12. **Krause GH, Weis E** (1984) Chlorophyll fluorescence as a tool in plant physiology. II. Interpretation of the fluorescence signals. Photosynth Res **5:** 139–157
13. **Krause GH, Vernotte C, Briantais JM** (1982) Photoinduced quenching of chlorophyll fluorescence in intact chloroplasts and algae. Resolution into two components. Biochim Biophys Acta **679:** 116–124
14. **Lavorel J, Etienne AL (1977)** *In vivo* chlorophyll fluorescence. *In* J Barber ed, Primary Processes of Photosynthesis. Elsevier/North-Holland Biomedical Press, Amsterdam, pp 203–268
15. **Ogren E, Baker NR** (1985) Evaluation of a technique for the measurement of chlorophyll fluorescence from leaves exposed to continuous white light. Plant Cell Environ **8:** 539–547
16. **Peltier G, Thibault P** (1985) O_2 uptake in the light in *Chlamydomonas*. Evidence for persistent mitochondrial respiration. Plant Physiol **79:** 225–230
17. **Peterson RB, Sivak MN, Walker DA** (1988) Relationship between steady-state fluorescence yield and photosynthetic efficiency in spinach leaf tissue. Plant Physiol **88:** 158–163
18. **Peterson RB, Sivak MN, Walker DA** (1988) Carbon dioxide-induced oscillation in fluorescence and photosynthesis. Role of thylakoid membrane energization in regulation of PSII activity. Plant Physiol **88:** 1125–1130
19. **Quick WP, Horton P** (1986) Studies on the induction of chlorophyll fluorescence changes in the level of glycerate-3-phosphate and the patterns of fluorescence quenching. Biochim Biophys Acta **849:** 1–6
20. **Schreiber U** (1986) Detection of rapid induction kinetics with a new type of high frequency modulated chlorophyll fluorometer. Photosynth Res **9:** 261–272
21. **Schreiber U, Bilger W** (1985) Rapid assessment of stress effects on plant leaves by chlorophyll fluorescence measurements. NATO Advanced Research Workshop. Springer-Verlag Berlin
22. **Schreiber U, Schliwa U, Bilger W** (1986) Continuous recording of photochemical and non-photochemical fluorescence quenching with a new type of modulation fluorometer. Photosynth Res **10:** 51–62
23. **Sharkey TD, Berry JA, Sage RF** (1988) Regulation of photosynthetic electron transport in *Phaseolus vulgaris* L., as determined by room temperature fluorescence. Planta **176:** 415–424
24. **Sivak MN, Walker D** (1985) Chlorophyll *a* fluorescence: can it shed light on fundamental questions in photosynthetic carbon dioxide fixation? Plant Cell Environ **8:** 439–448
25. **Strickland JDH, Parsons TR** (1972) A practical handbook of sea water analysis. Fisheries Research Board of Canada, Ottawa
26. **Turpin DH, Weger HG** (1988) Steady-state chlorophyll *a* fluorescence transients during ammonium assimilation by the *N*-limited green alga *Selenastrum minutum*. Plant Physiol **88:** 97–101
27. **Turpin DH, Elrifi IR, Birch DG, Weger HG, Holmes JJ** (1988) Interactions between photosynthesis, respiration, and nitrogen assimilation in microalgae. Can J Bot **66:** 2083–2097
28. **Walker DA, Sivak MN, Prinsley RT, Cheesbrough JK** (1983)

Simultaneous measurement of oscillations in oxygen evolution and chlorophyll *a* fluorescence in leaf pieces. Plant Physiol **73:** 542–549

29. **Weger HG, Turpin DH** (1989) Mitochondrial respiration can support NO_3^- and NO_2^- reduction during photosynthesis: interactions between photosynthesis, respiration and N assimilation in the *N*-limited green algae *Selenastrum minutum*. Plant Physiol **89:** 409–415
30. **Weger HG, Birch DG, Elrifi IR, Turpin DH** (1988) Ammonium assimilation requires mitochondrial respiration in the light. A study with the green alga *Selenastrum minutum*. Plant Physiol **86:** 688–692
31. **Weis E, Berry JA** (1987) Quantum efficiency of photosystem II in relation to energy dependent quenching of chlorophyll fluorescence. Biochim Biophys Acta **894:** 198–208
32. **Weis E, Ball JT, Berry JA** (1987) Photosynthetic control of electron transport in leaves of *Phaseolus vulgaris*: evidence for regulation of photosystem 2 by the proton gradient. *In* J. Biggins, ed., Progress in Photosynthesis Research, Vol 2. Martinus Nijhoff Publishers, Dordrecht, pp 553–556